Published online: December 30, 2019

Original Research

Long noncoding RNA-regulator of reprogramming alleviates hypoxia-induced cerebral injury in mice model and human via modulating apoptosis complexes

Qiong Zhou , Yangfang An and Yonghong Tang *

Department of Neurology, Yiyang Central Hospital, No. 336 Dongfengnan Road, Hengyang City, Hunan Province, 413000, P. R. China

*Correspondence: tyh1230@126.com (Yonghong Tang)

DOI:10.31083/j.jin.2019.04.1194

Ischemic stroke causes cerebral hypoxia, while long noncoding RNA regulator of reprogramming is associated with hypoxia. To find a new intervention target to protect hypoxic cerebral tissue and a potential biomarker from reflecting the severity of hypoxia after ischemic stroke, our research explored the expression pattern and function of the regulator of reprogramming in cerebral hypoxia-induced injury. The expression pattern and the function of the regulator of reprogramming were explored in mice with middle cerebral artery occlusion, and human brain microvascular endothelial cells underwent oxygen-glucose deprivation treatment. A case-control study, including 223 ischemic stroke patients and 155 controls were also conducted to investigate its correlation with ischemic stroke clinical characteristics. Results showed that the regulator of reprogramming increased significantly in middle cerebral artery occlusion in mice ($P < 0.05$), and its level remained stable within 2 to 48 h after the implement of middle cerebral artery occlusion. Oxygen-glucose deprivation up-regulated the expression of regulator of reprogramming, and regulator of reprogramming promoted ASK-1/STRAP/14-3-3 complex formation to inhibit the activation of TNF-α/ASK-1-mediated apoptosis of human brain microvascular endothelial cells, while small interfering ribonucleic acid (RNA) targeting regulator of reprogramming amplified these effects. Regulator of reprogramming increased and maintained stable within 3 to 48 h of ischemic stroke onset in patients, and was negatively associated with the National Institutes of Health Stroke Scale (NIHSS) (r = -0.708, $P < 0.001$), high sensitivity C-reactive protein (Hs-CRP) (r = -0.683, $P < 0.001$) level, infarct volume (r = -0.579, $P < 0.001$), and modified Rankin scale (mRS) (r = -0.728, $P < 0.001$). These results indicate that the regulator of reprogramming can alleviate cerebral hypoxia-induced injury by suppressing TNFα-induced apoptosis of vascular endothelial cells.

Keywords

Ischemic stroke; hypoxia; long non-coding RNA; the regulator of reprogramming; apoptosis complexes; mice model

1. Introduction

Post-Ischemic stroke (IS) brain injury is caused by a series of complex pathophysiological events, including excitotoxicity, oxidative and nitration stress, inflammation, and apoptosis. Apoptosis of vascular endothelial cells contributes to the development of acute ischemia of brain tissues. However, the mechanisms still wait to be elucidated. (Radak et al., 2017). IS leads to hypoxia of brain tissue, which has mechanism connections in changing brain response to ischemic injury (Seyed et al., 2017), and is also the main cause of morbidity and mortality of IS patients (Ma et al., 2017). Prevention and treatment for cerebral hypoxia after IS onset are of clinical importance. Despite the high incidence, the treatment of stroke injury is rare, partly due to the incomplete understanding of cellular and molecular changes that occur after IS (Catanese et al., 2017). Until now, the standard gold treatment for IS is still the tissue plasminogen activator thrombolysis (Knecht et al., 2017). However, the time-constrained therapeutic window was limited within 4.5 h after stroke onset, and the curative effect was not satisfactory when drugs were given after that time window (Knecht et al., 2017). Thus, a new therapeutic target for intervention and a non-invasive indicator to monitor disease severity are both crucial to improve the outcomes.

Recent documents had suggested an association between long non-coding RNA (lncRNA) and cardio-cerebrovascular disease (CCVD). Studies reported that lncRNAs were involved in several key processes of CCVD development, including the proliferation, migration, and angiogenesis of brain cells in oxygen-deficient environment (Ahmed et al., 2018; Wang et al., 2018), and also the lipid metabolism regulation during atherosclerosis development (Zeng et al., 2018). LncRNA regulator of reprogramming (ROR), which is located at 18q21.31 in chromatin, had been implied to have a strong susceptibility with CCVD (Li et al., 2019). Previous studies showed that the expression of ROR could be induced by oxygen-deficiency in liver tissue (Takahashi et al., 2014), cardiomyocytes (Wang and Yuan, 2019), and cortical neurons (Xu et al., 2014). Up-regulated expression of ROR could directly or indirectly activate mitogen-activated protein ki-

Journal of Integrative Neuroscience

nase/extracellular signal-regulated kinase (MAPK/ERK) pathway by interacting with other microRNAs, thus protected cells from hypoxia-caused injury (Ge et al., 2019; Zhang et al., 2019). Additionally, ROR can also modulate some apoptosis-related proteins to regulate cell proliferation and apoptosis (Yang et al., 2018). Apoptosis signal-regulating kinase 1 (ASK-1) is a key factor mediates diverse biological signals leading to cell death, through forming apoptosis complexes with other proteins and further activating c-Jun N-terminal protein kinase (JNK) and mitogen-activated protein kinase kinases (MAPK) pathways. ASK-1 had been shown to play a role in ischemic injury (Chikako, 2008).

In the present study, we suggest a hypothesis that ROR could be induced by IS onset and served as a protective factor to prevent brain tissue from the damage caused by hypoxia by regulating apoptosis complexes formation. To prove the hypothesis, oxygen-glucose deprivation (OGD) treatment in human brain microvascular endothelial cells (HBMECs) and middle cerebral artery occlusion (MCAO) in mice is performed to simulate the IS model. ROR expression pattern and its functions in cerebral hypoxia-induced injury are to be investigated. The correlation between the ROR level and the severity of IS is also analyzed in patients to find a new intervention target to protect hypoxic cerebral tissue and a potential biomarker from reflecting the severity of hypoxia after IS.

2. Materials and methods

2.1 Ethics approval

This project was all approved by the Ethics Committee of Yiyang Central Hospital (Hunan Province, P. R. China). Reference number: H201803043. Written informed consent was provided before sample collection. All animal experiments were approved by the Research Center for Medicine & Department of Laboratory Animal Science of Nanhua University. Reference number: 201506164.

2.2 MCAO model establishment

Thirty-six CD-1 mice (25-30 g, males) were purchased from the Research Center for Medicine & Department of Laboratory Animal Science of Nanhua University. Mice were randomly divided into the control group (n = 12), the sham group (n = 12), and the MCAO group (n = 12). In the MCAO group, 3% chloral hydrate (300 mg/kg, i.p.) was used to anesthetize the mice. Then a silicon-coated monofilament nylon suture was used to occlude the origin of MCA. B-ultrasound was used to detected mice's cerebral blood flow, and the successful MCAO modeling was confirmed by the reduction of hemispheres' blood flow. The sham group underwent the same anesthesia and surgical procedure except for the suture ligation of MCA. Mice in the control group did not receive any surgical operations. 40 μL vein blood was collected from the tail of each mouse at different times after modeling.

2.3 Cell culture and OGD treatment

HBMECs were cultured in high-glucose Dulbecco's Modified Eagle Medium (DMEM) (Gibco, USA) supplemented with 10% fetal bovine serum (FBS) (Gibco, USA) and 100 U/mL penicillin-streptomycin, and grew in an incubator in 37 °C with 5% CO_2. The culture was replaced every other day. OGD treatment was performed by culturing cells in DMEM containing no glucose (Gibco, USA), and incubating cells in an incubator (Thermo Scientific, USA) with 1% O_2, 5% CO_2, and 94% N_2 for different times. (Zhou et al., 2019).

2.4 Cell transfection

Negative control (NC) and three small interfering RNAs targeting ROR (si-ROR) were purchased from Genepharm. Co. (Shanghai, P. R. China). The sequences of siRNAs were provided in Supplementary (Table 1). Lipofectamine 3000 (Invitrogen, USA) was used to perform the transfections. Briefly, the original culture was removed and replaced with a culture containing a mixture of siRNAs and Lipofectamine 3000 (1 : 1). After 6 h of incubation, culture was replaced with normal medium containing no FBS. After 48 h of transfection,, ROR expression was detected. The silencing efficiency was evaluated by the down-regulation of ROR at 48 h post-transfection. In this study, si-ROR-3 was finally used to silence ROR expression.

2.5 Western blot analysis

Cells were lysed on ice and centrifuged at 12,000 g for 5 min to separate cell debris. Total protein concentration was detected by the BCA method (BCA Protein Assay Kit, Beyotime, P. R. China). Then equal amount of proteins from each group were separated on 10% SDS-PAGE gels and transferred onto a polyvinyl difluoride (PVDF) membrane. After incubated with 5% BSA (Bovine Serum Albumin) at 37 °C for 1 h, the membrane was incubated with one of the following antibodies overnight at 4 °C: anti-Bax antibody (ab32503, Abcam), anti-ASK-1 antibody (8662, Cell Signaling Technology), anti-phospho-ASK-1 antibody (3764, Cell Signaling Technology), anti-STRAP antibody (AP29336; One World Lab), anti-14-3-3 antibody (9636; Cell Signaling Technology), anti-caspase 8 antibody (ab25901, Abcam), anti-TNF-α antibody (ab1793, Abcam), and anti-tubulin antibody (ab6160, Abcam). Then the membrane was incubated with secondary antibody (ab6721 or ab6789, Abcam) for 1 h at room temperature. Finally, the membrane was photographed by ECL Imaging System (Tanon 6060, USA).

2.6 Flow cytometry

Annexin V fluorescein isothiocyanate (FITC)/apoptosis detection kit (Sigma, USA) was used to evaluate cell apoptosis according to the manufacturers' instructions. Briefly, 5 μL annexin V-FITC and 10 μL propidium iodide were added to cell suspensions and incubated for 15 min at room temperature. Then stained cells were analyzed by BD FACS Calibur™ flow cytometer (BD Biosciences, USA).

2.7 Immunofluorescence

Cells were washed with cold phosphate buffered saline (PBS) twice and fixed with 4% polyoxymethylene for 10 min at room temperature. Then cells were incubated with 52-(4-Amidinophenyl)-6-indolecarbamidine dihydrochloride (DAPI) was added and incubated for another 2 min to indicate the nucleus. Finally, cells were washed twice using PBS and were observed under an inverted microscope (Olympus, Japan).

2.8 Apoptosis complexes isolation

Lysates were generated from the brain tissues of ICR mice. The lysates were precleared with Protein G beads in advance. After that, the precleared lysates were incubated with 5 μg/mL of anti-ASK-1 antibody (8662; Cell Signaling Technology), or anti-P-

Table 1. Characteristics of participants

Subject groups	Quartiles of ROR, range, relative expression (-log), N = 378				*P*
	1st, < 1.931	2nd, 1.931-2.445	3rd, 2.445-3.278	4th, > 3.278	
LAA	59 (62.43%)	23 (24.34%)	11 (11.64%)	8 (8.47%)	< 0.001
CE	11 (11.64%)	14 (14.81%)	15 (15.87%)	13 (13.75%)	0.513
SVO	17 (18.00%)	18 (19.05%)	18 (19.05%)	17 (18.00%)	0.919
Control	13 (13.76%)	32 (33.86%)	56 (59.26%)	54 (57.14%)	< 0.001

Abbreviation: CE: cardioembolism; LAA: large-artery atherosclerosis; SVO: small vessel occlusion.

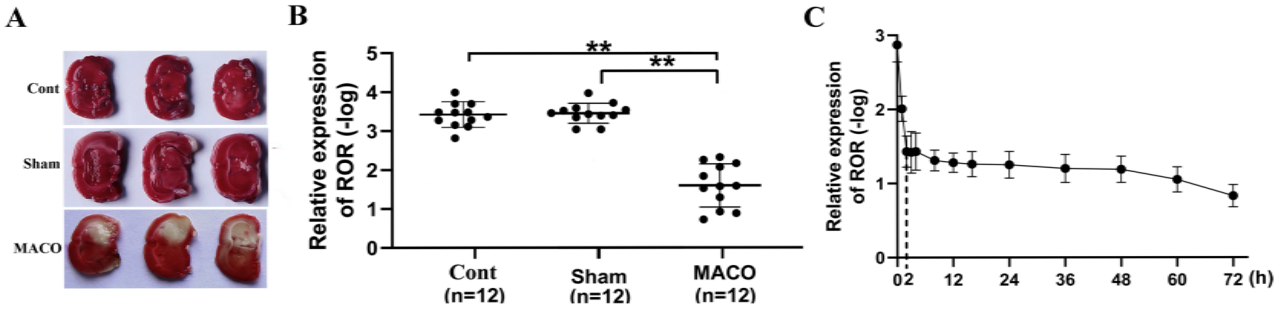

Figure 1. The expression pattern of ROR in MCAO mice. (A). Mouse brain tissue after MCAO establishment. (B). ROR level in the MCAO group was up-regulated significantly compared to that in the sham group and the control group at 24 h after the IS model establishment. (C). ROR expression pattern during IS model establishment. Data are shown as mean ± SEM, $^{**}P < 0.001$.

ASK-1 antibody (28201-1-AP, protein tech group) to pull down the target complexes. Normal rabbit IgG (5 μg/mL) was also added as a negative control. All samples were incubated overnight using a constant rotation at 4 °C. Then protein G beads were added and incubated for another 2 h. After washed 6 times by 1 × lysis buffer, protein G beads were boiled in 1 × loading buffer, and the co-precipitated complexes were then separated on SDS-PAGE and used for Western blotting analysis.

2.9 Human study subjects

Two hundred and twenty-three patients (145 men and 78 women, mean age: 67.76 ± 6.32) diagnosed as IS between December 2015 and April 2018 at Yiyang Central Hospital, Hunan, P. R. China, were recruited in this study. Patients were classified into three groups: large-artery atherosclerosis (LAA), cardioembolism (CE), and small-vessel occlusion (SVO) according to the results of magnetic resonance imaging and computed X-ray tomography. At admission, the National Institutes of Health Stroke Scale (NIHSS) score, the infarct volume, and the high sensitivity C-reactive protein (Hs-CRP) were all assessed. The modified Rankin Scale (mRS) of subjects was recorded 6 months after hospitalization. One hundred fifty-five controls (104 men and 51 women, mean age: 65.53 ± 7.98) from the health examination center were also collected. For IS patients, blood samples were collected at different times after symptom onset (within 3-12 [n = 64], 12-24 [n = 116], 24-36 [n = 32], 36-48 [n = 11]). For healthy controls, blood samples were all obtained at the time of physical examination.

2.10 Quantitative real-time PCR (qRT-PCR)

Total RNA was extracted by Invitrogen™ TRIzol™ Reagent (Thermo Fisher Scientific, USA). The concentration of total RNA was detected by Nanodrop 2000 (Thermo, USA). RNA was reverse transcribed into cDNA using PrimeScriptTM RT Master Mix (Takara, Japan). ROR expression was detected on the Bio-Rad CFX96 (Inc., Hercules, CA, USA) using SYBR Green qPCR Mix (CWBIO, P. R. China). The sequence of primers was provided in Supplementary (Table 1). Two control transcripts, β-actin, and GAPDH were both detected in this study. Compared to β-actin, the intra- and inter-group variabilities of GAPDH expression were smaller, so GAPDH was finally chosen as the control. The expression of ROR was normalized to GAPDH. All experiments were in triplicates. ROR level was calculated using the 2-ΔCT method, where ΔCT = CT(target) - CT(reference).

2.11 Statistical analysis

SPSS version 20.0 was used to perform statistical analyses. In this study, normally distributed data were presented as mean ± standard deviation (M ± SD), while skewed data were presented as median (interquartile range, IQR). For normally distributed variables, Student's *t*-test was used to evaluate the difference between the two groups, and one-way ANOVA was used for the analysis of multiple groups. Categorical variables were analyzed by the χ^2 test. Correlations were analyzed using Pearson or Spearman correlation analysis. In respect to animal experiments and human study, the group information as defined by numbers and staff who were responsible for data collection and data analysis were all blind to the status of subjects. In this study, $P < 0.05$ was considered to be statistically significant.

3. Results

3.1 MACO mice had elevated ROR expression level

Fig. 1A shows mice brain images after MCAO operation. Brain tissue in the MACO group showed a significant pale region caused by ischemia. Results showed that ROR expression in mice from

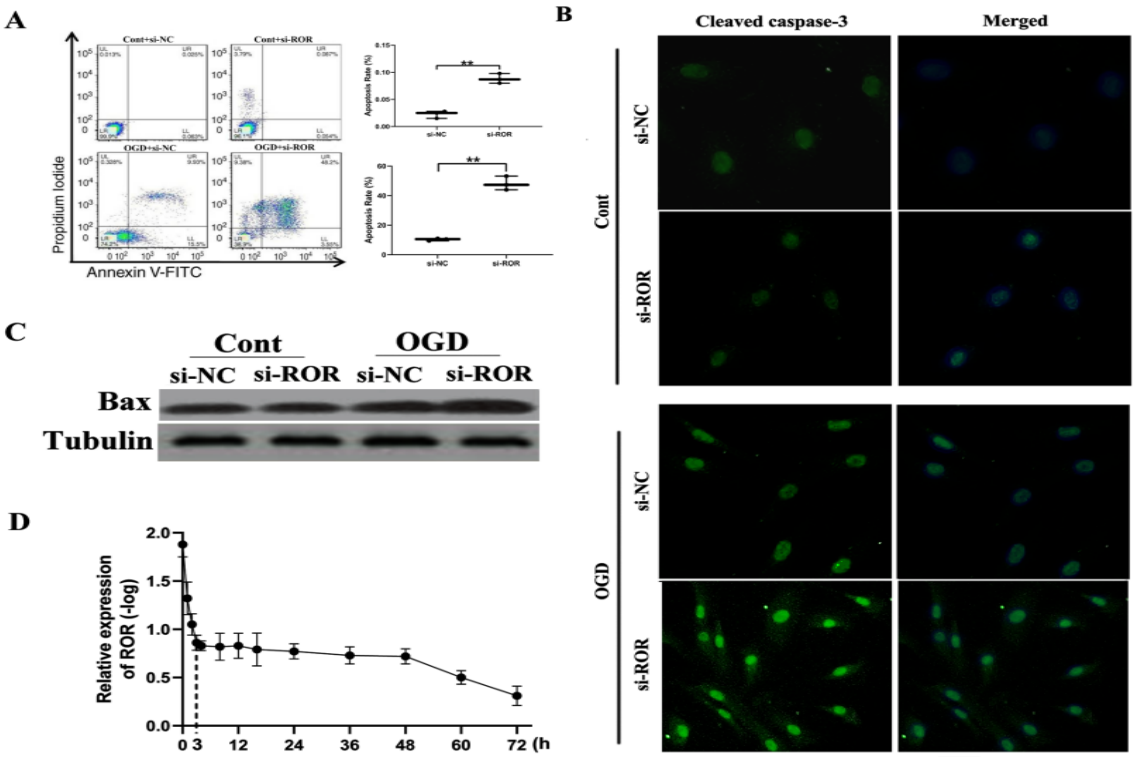

Figure 2. Apoptosis of HBMECs in different groups. (A). Results of flow cytometry showed that apoptosis of HBMECs was significantly up-regulated in response to si-ROR treatment. (B). Results of western blot showed that OGD significantly up-regulated Bax expression, and this effect can be amplified by si-ROR. (C). Results of immunofluorescence showed that OGD significantly up-regulated cleaved caspase-3 expression, and this effect can be amplified by si-ROR. (D).The expression pattern of ROR after OGD treatment. Data are shown as mean ± SEM, $**P < 0.001$.

the MCAO group was markedly increased compared to that in the sham group and the control group, while there's no significant difference between ROR level in mice from the control group and the sham group (Fig. 1B). The expression of ROR after MACO establishment rapidly raised in the first 2 h, then kept stable within 2 to 48 h, and shows a slow-upward trend after 48 h (Fig. 1C).

3.2 ROR inhibited apoptosis of HBMECs

We further detected the expression levels of some apoptosis-related proteins. As the results showed, expressions levels of Bax and cleaved caspase-3 significantly increased after OGD treatment, as well as the apoptosis rate of HBMECs, while si-ROR amplified these effects (Fig. 2A, B, C). Besides, ROR expression in HBMECs could also be up-regulated by OGD treatment, whose expression pattern was similar to that in MACO mice: increased rapidly in the first 3 h, then remained stable and gradually increased within 3 to 48 h (Fig. 2D).

3.3 ROR enhanced ASK-1/STRAP/14-3-3 complex formation and inhibited the activation of TNF-α/P-ASK-1-mediated apoptosis

We further analyzed the apoptosis complexes in different groups. The results showed that OGD treatment could significantly promote the combination of STRAP and 14-3-3 to ASK-1, thus inhibited the interaction of TNF-α and P-ASK-1. In other words, OGD treatment to HBMECs promoted ASK-1/STRAP/14-3-3 complex formation and inhibited TNF-α/P-ASK-1 complex formation, while si-ROR amplified these effects (Fig. 3A, B).

3.4 ROR expression in serum was elevated in IS patients

ROR level in IS patients went to the hospital at different times after IS onset was analyzed, and no significant difference was observed ($P > 0.05$, Fig. 4A). However, we did observe that IS patients had significantly higher ROR expressions compared to controls ($P < 0.001$, Fig. 4B), which is consistent with the results from the animal study and cell study. Further research showed that patients in the LAA group had the highest ROR expressions compared with patients in CE, SVO, and control groups, while there's no significant difference in ROR expressions between CE and SVO group (Fig. 4C).

3.5 ROR expression and clinical characteristics

To evaluate the value of ROR in reflecting disease severity of IS, we further analyzed the correlation between serum ROR expression level and the clinical characteristics of IS patients. As the results showed, ROR expression level was negatively correlated with NIHSS scores (r = -0.708, $P < 0.001$, Fig. 5A), infarct volume (r = -0.579, $P < 0.001$, Fig. 5B), and Hs-CRP level (r = -0.683, $P < 0.001$, Fig. 5C). Also, there was a significant negative correlation between serum ROR expression level and mRS score (r = -0.728, $P < 0.001$, Fig. 5D).

4. Discussion

We found that the level of ROR can be acutely up-regulated in hypoxia status caused by IS, and its level within 3-48 h of the onset of IS is negatively correlated with the severity of the disease.

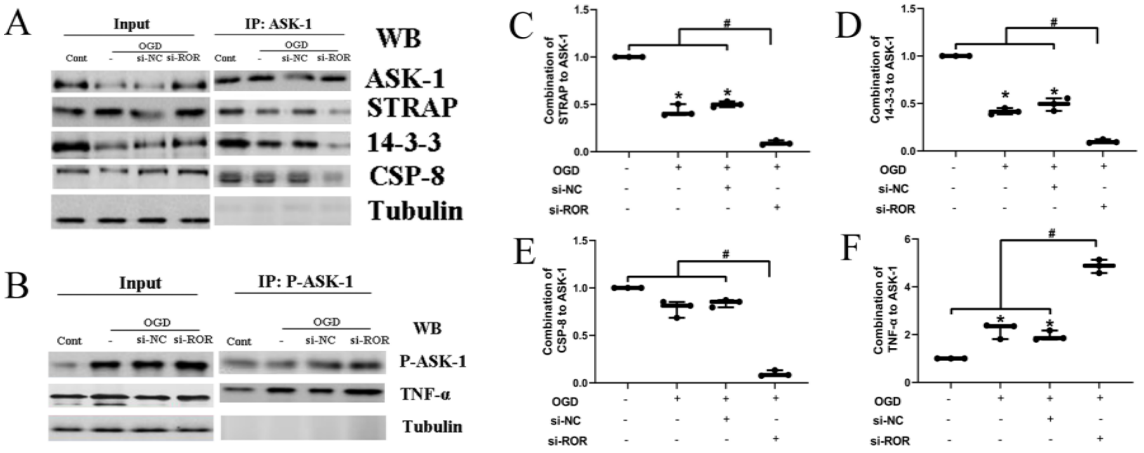

Figure 3. Apoptosis complexes of HBMECs in different groups. (A. C. D. E). OGD treatment significantly reduced ASK-1/STRAP/14-3-3 complex formation, and si-ROR amplified these effects. (B. F) OGD treatment enhanced the formation of TNF-α/P-ASK-1 complexes, and si-ROR amplified these effects. Data are shown as mean $\pm$ SEM, $*P < 0.05$, $\#P < 0.001$.

The underlying mechanism may be that ROR promoted ASK-1/STRAP/14-3-3 complex formation to inhibit the activation of TNF-α/P-ASK-1-mediated apoptosis of vascular endothelial cells.

Regarding the potential mechanism of IS development, the underlying mechanisms are still not fully understood. Brain ischemia may lead to IS. In the process of IS, the brain tissue has two important independent areas: ischemic core area and ischemic penumbra. The core of cerebral ischemia experienced a sudden decrease in blood flow within minutes after the ischemic attack, accompanied by irreversible damage and subsequent cell death. On the other hand, apoptosis in ischemic penumbra may occur in hours or days, while necrosis begins in the first hour after the onset of IS. IS is characterized by key molecular events that initiate apoptosis in many cells, such as excessive production of free radicals, Ca^{2+}overload, and excitotoxicity. These changes in intracellular homeostasis may lead to necrosis and apoptosis, usually depending on cell type, cell age, and the area of the brain. Apoptosis leads to DNA breakage, cytoskeleton and nucleoprotein degradation, protein cross-linking, apoptotic body formation, phagocyte receptor expression or ligand expression, and finally phagocyte absorption (Djordje et al., 2017). Therefore, apoptosis is the key event mediating IS-induced cerebral injury. In this point, reversing the apoptosis process may be the key way to protect brain tissue from the damage caused by hypoxia. For this purpose, numerous studies had explored the possible factors which served as the protectors to prevent hypoxia-caused cerebral injury.

Blood vessels act as conduits for O(2) and nutrients. Microvascular endothelial cells are most sensitive to hypoxia. After IS onset, hypoxia-inducible factor-1 (HIF-1) mediates the adaptive transcription response to hypoxia/ischemia in microvascular endothelial cells, which leads to the expression changes of thousands of genes and non-coding RNAs (Gregg, 2010). ROR had drawn interest because of its function in the reprogramming in cardiac hypertrophy (Jiang et al., 2016). And recently, the elevated level of ROR was proved to be associated with the hypoxia damage. ROR expression was up-regulated in ischemia patients, and hypoxia treated human cardiomyocytes (Zhang et al., 2018).

Additionally, ROR could decrease cell viability, inhibit apoptosis by regulating apoptosis-associated factor expressions via the p38/MAPK signaling pathway (Zhang et al., 2018). In our study, we found that ROR expression could be induced by MACO and OGD treatment, and with the treatment time prolonged, the higher expression level of ROR was observed. That means, ROR level may reflect the severity of ischemia, and this is verified by the results that the ROR level was negatively correlated with NIHSS scores, Hs-CRP levels, and infarct volume in IS patients. Also, serum ROR level was found to be negatively correlated with the mRS scores at 6 months after IS onset, which indicated a potential prognostic value of ROR.

We have shown that ROR acted as a protective factor to reduce the damage caused by hypoxia. On the one hand, highly expressed ROR interacts with other non-coding RNAs, such as miR-145 and miR-377, to regulate cell proliferation and apoptosis (Zhou et al., 2016, 2019), whereby ROR can also directly regulate expressions of apoptosis-related proteins, including Bax and cleaved caspase-3, and further inhibits the apoptosis of cells (Yang et al., 2018). Apoptosis of vascular cells contributes to the arterial architecture, especially when coordinated with matrix turnover and proliferation of vascular cells. Furthermore, studies have proven that ROR was also involved in vascular cell proliferation by regulating the expression of vascular endothelial growth factor (Shi et al., 2019). These results all indicate that ROR might be used as an agent to reverse vascular damage.

We also found that ROR could promote ASK-1/STRAP/14-3-3 complex formation to inhibit the activation of TNF-α/P-ASK-1-mediated apoptosis of the vascular endothelial cell. ASK-1 is a component of TNF-α-induced apoptosis complex I, and its activation (phosphorylation) is required for TNF-α-induced apoptosis in multiple cell types to prevent TNF-α-induced apoptosis, STRAP and 14-3-3 proteins interact with ASK-1 to disrupt associations between TNF receptor-associated factor 2 and ASK-1 upon TNF-α stimulation (Han et al., 2015; Hatai et al., 2000). We found that OGD treatment promoted ASK-1/STRAP/14-3-3 complex formation and inhibited TNF-α/P-ASK-1-mediated apoptosis of vascular endothelial cells, while si-ROR amplified these effects. These data implied that ROR might be a new intervention target to al-

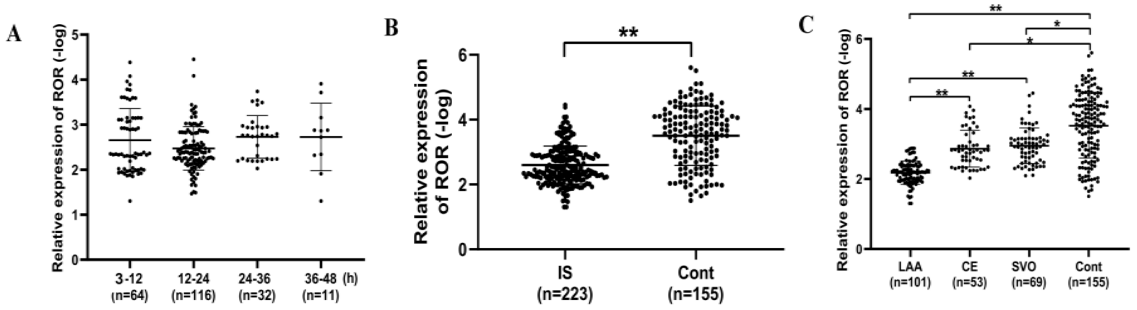

Figure 4. Serum ROR expression in different groups. (A). No significant difference was found in ROR expression among patients admitted to hospital at different times. (B). Compared to controls, ROR expression was up-regulated significantly in IS patients. (C). ROR expression in large-artery atherosclerosis (LAA) was up-regulated most significantly. Data are shown as mean ± SEM, $*P < 0.05$, $**P < 0.001$.

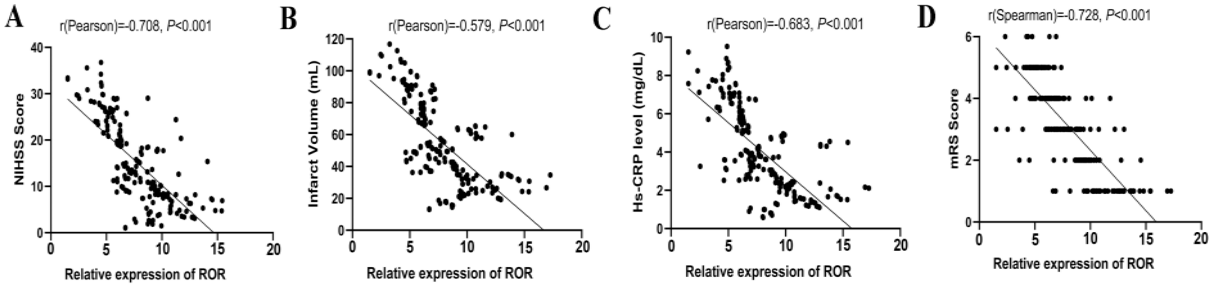

Figure 5. Relationship between serum ROR level and the severity of IS. (A) Serum ROR level had a positive correlation with the National Institutes of Health Stroke Scale (NIHSS) score of IS patients. (B) Serum ROR level had a positive correlation with the infarct volume. (C) Serum ROR level had a positive correlation with serum Hs-CRP. (D) Serum ROR level had a positive correlation with the modified Rankin Scale (mRS) score.

leviate the apoptosis of vascular endothelial cells and to relieve cerebral hypoxia.

5. Conclusions

In conclusion, we found that ROR expression was rapidly increased and kept a stable value within 3 to 48 h after IS onset. We also observed that serum ROR expression was negatively correlated with the severity of IS. The potential mechanism may be that hypoxia stimulated the expression of ROR, and ROR further enhanced ASK-1/STRAP/14-3-3 complex formation to inhibit the activation of TNF-α/P-ASK-1-mediated apoptosis in vascular endothelial cells, thus alleviates hypoxia in brain tissue. Moreover, we have found that ROR expression showed a quick change within 3 h after IS onset and remained a stable level within 3 to 48 h. This provides us plenty of time to diagnose patients, and it also suggests that detecting ROR in IS patients is feasible and credible. These findings indicate that ROR could serve as an invention target for IS therapy, and peripheral blood ROR may be used as a novel marker to reflect the severity and to predict the prognosis of IS.

Authors' contributions

YT developed the hypothesis and designed the research. QZ and YA executed the experiments. QZ participated in data analysis and manuscript writing up.

Acknowledgments

We thank all of the subjects enrolled in this study.

Conflict of interest

The authors declare no conflict of interest exists.

Submitted: September 26, 2019
Accepted: November 14, 2019
Published: December 30, 2019

References

Ahmed, A. S. I., Dong, K., Liu, J., Wen, T., Yu, L., Xu, F., Kang, X., Osman, I., Hu, G., Bunting, K. M., Crethers, D., Gao, H., Zhang, W., Liu, Y., Wen, K., Agarwal, G., Hirose, T., Nakagawa, S., Vazdarjanova, A. and Zhou, J. (2018) Long noncoding RNA NEAT1 (nuclear paraspeckle assembly transcript 1) is critical for phenotypic switching of vascular smooth muscle cells. *Proceedings of the National Academy of Sciences of the United States of America* **115**, e8660-e8667.

Catanese, L., Tarsia, J. and Fisher, M. (2017) Acute Ischemic Stroke Therapy Overview. *Circulation Research* **120**, 541-558.

Chikako, H. (2008) Role of Apoptosis Signal-Regulating Kinase 1 (ASK 1)-mediated Signaling pathway during ischemic retinal injury. *Nippon Ganka Gakkai Zasshi* **112**, 965-974. (In Japanese)

Djordje, R., Niki, K., Ivana, R., Aleksandra, J., Emina, S., Sonja, Zafirovic., Shaker, A. M. and Esma, R. I. (2017) Apoptosis and Acute Brain Ischemia in Ischemic Stroke. *Current Vascular Pharmacology* **15**, 115-122.

Ge, H., Liu, J., Liu, F., Sun, Y. and Yang, R. (2019) Long non-coding RNA ROR mitigates cobalt chloride-induced hypoxia injury through regulation of miR-145. *Artificial Cells Nanomedicine and Biotechnology* **47**, 2221-2229.

Gregg, L. S. (2010) Vascular responses to hypoxia and ischemia. *Arteriosclerosis, Thrombosis, and Vascular Biology* **30**, 648-652.

Han, S. J., Jung, S. Y., Wu, S. P., Hawkins, S. M., Park, M. J., Kyo, S., Qin, j., Lydon, J. P., Tsai, S. Y., DeMayo, F. J. and O'Malley, B. W. (2015)

Estrogen receptor β modulates apoptosis complexes and the inflammasome to drive the pathogenesis of Endometriosis. *Cell* **163**, 960-974.

Hatai, T., Matsuzawa, A., Inoshita, S., Mochida, Y., Kuroda, T., Sakamaki, K., Kuida, K., Yonehara, S., Ichijo, H. and Takeda, K. (2000) Execution of apoptosis signal-regulating kinase 1 (ASK1)-induced apoptosis by the mitochondria-dependent caspase activation. *The Journal of Biological Chemistry* **275**, 26576-26581.

Jiang, F., Zhou, X. and Huang, J. (2016) Long Non-Coding RNA-ROR Mediates the Reprogramming in Cardiac Hypertrophy. *PLoS One* **11**, e0152767.

Knecht, T., Story, J., Liu, J., Davis, W., Borlongan, C. V. and Dela, Peña. I. C. (2017) Adjunctive therapy approaches for ischemic stroke: innovations to expand time window of treatment. *International Journal of Molecular Sciences* **18**, e2756.

Li, S., Yue, X. C. and Sun, C. Y. (2019) Prognostic value of long noncoding RNA ROR in patients with cancer in China: A systematic review and meta-analysis. *Medicine (Baltimore)* **98**, e15758.

Ma, Y. L., Zhang, L. X. and Liu, G. L. (2017) N-Myc downstream-regulated gene 2 (Ndrg2) is involved in ischemia-hypoxia-induced astrocyte apoptosis: a novel target for stroke therapy. *Molecular Neurobiology* **54**, 3286-3299.

Radak, D., Katsiki, N. and Resanovic, I. (2017) Apoptosis and acute brain ischemia in ischemic stroke. *Current Vascular Pharmacology* **15**, 115-122.

Seyed, E. K., William, W., Maryam, F., Yaghoob, F. and Hadi, F. M. (2017) Pathogenic mechanisms following ischemic stroke. *Neurological sciences* **38**, 1167-1186.

Shi, J., Zhang, D., Zhong, Z. and Zhang, W. (2019) lncRNA ROR promotes the progression of renal cell carcinoma through the miR-206/VEGF axis. *Molecular Medicine Reports* **20**, 3782-3792.

Takahashi, K., Yan, I. K. and Haga, H. (2014) Modulation of hypoxia-signaling pathways by extracellular linc-RoR. *Journal of Cell Science* **127**, 1585-1594.

Wang, P. and Yuan, Y. (2019) LncRNA-ROR alleviates hypoxia-triggered damages by downregulating miR-145 in rat cardiomyocytes H9c2 cells. *Journal of Cellular Physiology* **234**, 23695-23704.

Wang, Z., Wang, R., Wang, K. and Liu, X. (2018) Upregulated long non-coding RNA Snhg1 promotes the angiogenesis of brain microvascular endothelial cells after oxygen-glucose deprivation treatment by targeting miR-199a. *Canadian Journal of Physiology and Pharmacology* **96**, 909-915.

Xu, D. M., Zhang, X. Y. and Wang, X. R. (2014) Antioxidative effects of cysteinyl leukotriene receptor antagonists montelukast and HAMI 3379 on ischemic injury in rat cortical neurons in vitro. *Zhejiang Da Xue Xue Bao Yi Xue Ban* **43**, 257-264. (In Chinese)

Yang, Z., Tang, Y., Lu, H., Shi, B., Ye, Y., Xu, G. and Zhao, Q. (2018) Long non-coding RNA reprogramming (lncRNA-ROR) regulates cell apoptosis and autophagy in chondrocytes. *Journal of Cellular Biochemistry* **119**, 8432-8440.

Zeng, Y., Ren, K., Zhu, X., Zheng, Z. and Yi, G. (2018) Long Noncoding RNAs: Advances in Lipid Metabolism. *Advances in Clinical Chemistry* **87**, 1-36.

Zhang, H. Y., Liang, F., Zhang, J. W., Wang, F., Wang, L. and Kang, X. G. (2017) Effects of long noncoding RNA-ROR on tamoxifen resistance of breast cancer cells by regulating microRNA-205. *Cancer Chemother Pharmacol* **79**, 327-337.

Zhang, W., Li, Y. and Wang, P. (2018) Long non-coding RNA-ROR aggravates myocardial ischemia/reperfusion injury. *Brazilian Journal of Medical and Biological Research* **51**, e6555.

Zhang, Z., Li, H., Liu, M., He, J., Zhang, X. and Chen, Y. (2019) Skullcapflavone I protects cardiomyocytes from hypoxia-caused injury through up-regulation of lincRNA-ROR. *International Journal of Immunopathology and Pharmacology* **33**, 1-11.

Zhou, P., Sun, L., Liu, D., Liu, C. and Sun, L. (2016) Long non-coding RNA lincRNA-ROR promotes the progression of colon cancer and holds prognostic value by associating with miR-145. *Pathology & Oncology Research* **22**, 733-740.

Zhou, Z. W., Zheng, L. J., Ren, X., Li, A. P. and Zhou, W. S. (2019) LncRNA NEAT1 facilitates survival and angiogenesis in oxygen-glucose deprivation (OGD)-induced brain microvascular endothelial cells (BMECs) via targeting miR-377 and upregulating SIRT1, VEGFA, and BCL-XL. *Brain Research* **1707**, 90-98.